



Comparison of the welding deformation of mismatch and normal butt joints produced by laser-arc hybrid welding

Liqun Li^a, Hongbo Xia^{a,*}, Ninshu Ma^{b,*}, Bo Pan^a, Yichen Huang^a, Shuai Chang^a

^a State Key Laboratory of Advanced Welding and Joining, Harbin Institute of Technology, 92 West Dazhi street, Harbin, 15001, China

^b Joining and Welding Research Institute, Osaka University, 11-1 Mihogaoka, Ibaraki, Osaka, 567-0047, Japan

ARTICLE INFO

Keywords:

Laser-arc hybrid welding
Mismatch
Welding deformation
Inherent deformation
Pipe structure

ABSTRACT

A reliable numerical model is developed to predict the deformation of mismatch and normal butt-welded joints after laser and gas metal arc hybrid welding (Laser-GMAW). A smaller deflection is produced in the mismatch joint as a result of a more uniform weld profile along the thickness direction, while a larger shrinkage deformation is obtained as a result of the higher heat input compared to the normal joint. The transverse plastic strain is much larger than the longitudinal plastic strain for both joints. An interruption is observed at the bottom surface of the mismatch joint owing to the discontinuity of the weld profile. The calculated inherent deformation, based on the plastic strain, is much larger along the transverse direction than along the longitudinal direction and it is also the dominating welding deformation. The deformation of a pipe assembled with a longitudinal welding line is predicted from the calculated inherent deformation parameters. A smaller roundness (ΔR) and deflection (ΔZ) are produced in the mismatch joint due to its smaller inherent bending deformation compared to the normal joint.

1. Introduction

Laser-arc hybrid welding is increasingly studied due to its great penetration depth and relatively high welding speed [1]. For instance, Bunaziv et al. [2] obtained a fully penetrated 45 mm thick steel plate by double-side laser-arc hybrid welding at a welding speed of 1.2 m/min. In addition, the laser-arc hybrid approach allows selecting the assembling conditions, such as the welding gaps and energy ratios [3–6]. Therefore, the laser-arc hybrid welding technology has great potential to join steel for shipbuilding [7,8].

Numerical simulations of the laser-arc hybrid welding process are of importance as they not only allow visualizing the welding process but also provide a more economical way to optimize the welding parameters. The numerical description of the laser-arc hybrid heating source, the behavior of the molten pool, and the heat transfer during the process have been investigated. Xu et al. [9] optimized a numerical model of a laser and pulsed GMAW hybrid heating source. The optimized heating source was employed to simulate the thermal cycles during the Laser-GMAW process of a 6 mm–12 mm thick plate. The numerical results exhibited good agreement with experimental results. Piekarska et al. [10] investigated the factors affecting the weld profile during the laser-arc hybrid welding of 5 mm thick S355 steel by numerical simulations. They found that the geometry of the top surface of

the weld profile was mainly determined by the arc. Atabaki et al. [11] developed a model to elucidate the influence of the welding parameters on the stability of the arc during the laser-arc hybrid welding of 2.5 mm thick aluminum alloy plates with a T-joint configuration. They found that the stability of the arc could be improved by optimizing the vertical distance between the arc torch and the laser. This higher arc stability could be beneficial for obtaining a uniform and stable molten pool.

Simulations of the distribution of the welding residual stress, plastic strain, and deformation after laser-arc hybrid welding have also been investigated. Kong et al. [12] studied the influence of the welding speed on the residual stress during the laser-arc hybrid welding of 6 mm thick A36 carbon steel. They found that a higher welding speed could contribute to the reduction of the residual stress. This was in a good agreement between numerical results and results obtained by X-ray diffraction. Ma et al. [13] researched the influence of energy ratios between arc and laser RAQL (RAQL = 0.58, 1.13, 1.82) on the welding deformation. They found that the shrinkage deformation increases with the increase of RQALs due to higher heat input and that the largest deflection deformation was produced in the middle energy ratio (RQAL = 1.13) due to the largest difference in the weld profile along the thickness direction. Derakhshan et al. [14] studied the evolution of the residual stress during arc and laser-arc hybrid welding processes. They found that the residual stress changes to tensile stress with

* Corresponding authors.

E-mail addresses: jssrxhb@126.com (H. Xia), ma.ninshu@jwri.osaka-u.ac.jp (N. Ma).

increasing welding speed during laser-arc hybrid welding but remains compressive during arc welding.

In the practical process of laser-arc hybrid welding of a large structure, a geometrical mismatch will be generated by the assembling error or induced by existing weld seams. For instance, Wang et al. [15] calculated the welding deformation in a spherical structure assembled by 14 weld seams. They found that a radial deformation would be generated after the first welding line was conducted. This radial deformation would obviously cause the assembling mismatch in the subsequent welding processes. Petring et al. [16] found that the assembling mismatch has a significant influence on the shape of the weld profile, which would finally result in different distributions of the residual stress, plastic strain, and deformation compared with that of a normal joint. Although fit-ups can be employed in the welding process to reduce welding deformation, the deformation is not totally eliminated. Therefore, an assembling mismatch would be generated in the subsequent welding processes, which would change the final welding deformation regulation. Nevertheless, research on the influence of the assembling mismatch on the distribution of the plastic strain and deformation in mismatch butt-welded joints (simplified to mismatch joints hereafter) is rarely reported.

The aim of this study is to investigate the influence of the assembling mismatch on the welding deformation and plastic strain during the Laser-GMAW hybrid welding of 6 mm thick steel SS400 plates. First, a numerical model is developed to simulate the Laser-GMAW hybrid welding of the plates with mismatch and normal butt-welded joints (simplified to normal joints hereafter). Then, the deformation and plastic strain are extracted and compared, and inherent theory is adopted to analyze the deformation mechanism. Finally, the deformation of a pipe structure is predicted and compared based on the calculated inherent deformation parameters.

2. Research method

2.1. Experimental methods and welding conditions

In this study, a Laser-GMAW system, assembled from an IPG YLR-5000 (CW) Continuous Wave fiber laser with a 5 kW maximum laser power and a FRONIUS TPS4000 MIG welding equipment, was adopted. The Laser-GMAW system is presented in Fig. 1, and the detailed parameters of the system are listed in Table 1. A 1.2 mm mismatch distance was employed based on the calculated deformation of Laser-GMAW steel SS400 plates obtained by Ma et al. [13] (the same dimensions of the steel plate and similar welding parameters were adopted in this study). A slightly higher arc power was adopted for the mismatch joint (3875 W) than for the normal joint (3375 W) to guarantee the full

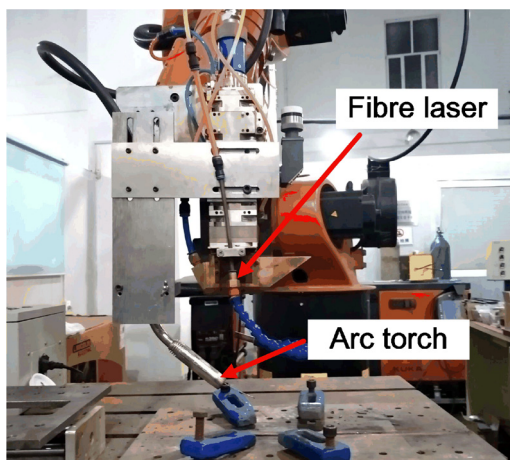


Fig. 1. Laser-GMAW hybrid welding system.

Table 1

Welding parameters for the mismatch and normal joints.

Joint characteristics	Total power (W)	Laser power (W)	Arc power (W)	Welding speed (mm/s)	Distance between laser and arc (mm)
Normal joint	6875	3500	3375 (135 A × 25 V)	16.7	4
Mismatch joint	7375	3500	3875 (155 A × 25 V)	16.7	4

penetration of base metals in the mismatch joint owing to its larger thickness. Before the Laser-GMAW process of the mismatch and normal joints, a Y-shape groove with a 45° angle was fabricated in the base metal, and a 0.6 mm gap was set between the roots of the base metals to ensure the smooth flow of fusion metals, as seen in Fig. 2.

2.2. Model description

Fig. 3 shows the dimensions and boundary conditions of the numerical model. The model has the same dimensions as the experimental workpiece (400 mm × 240 mm × 6 mm). Six degrees of freedom (DOF) of the nodal displacement were constrained to prevent the rigid motion of the workpiece during the Laser-GMAW process. The generated mesh for the mismatch and normal joints are presented in Fig. 4. Fig. 4(a) and (b) show the whole meshes for the mismatch and normal joints, respectively, and Fig. 4(c) and (d) show the meshes for the fusion zone and the nearby heat-affected zone (HAZ), respectively. To shorten the calculation times while maintaining acceptable accuracy, finer meshes (mesh size of about 0.5 mm) were divided in the fusion zone and the nearby HAZ, while coarser meshes were divided in the outer region. The thermal elastic-plastic finite element method (FEM) and the research software JWRIAN developed by Osaka University were adopted.

2.3. Material properties and heat sources

The mid carbon steel SS400 used for general structures (SS400 Japanese Standard; Q235 Chinese Standard) was selected as the base metal. The properties of the material and their evolution with temperature in the numerical simulation are shown in Table 2 [13].

The heat source in the Laser-GMAW process includes both the arc and the laser. Therefore, a mixed heat source model, including the distributions of both the arc and laser energy, was adopted. The arc and laser will interact with each other during the laser-arc hybrid welding process [17]. Therefore, the absorption efficiency of the arc and laser are different. According to the results obtained by Bang et al. [18], the energy efficiency of the laser and arc during laser-arc hybrid welding are 0.85 and 0.21, respectively. The energy distribution of the laser-arc hybrid heat source consists of two parts [19]: the arc, which is expressed by Eq. (1), and the laser, which is described by Eq. (2):

$$q_{arc}(x, y, z) = 6\sqrt{3} \frac{\eta_{arc} UI}{\pi \sqrt{\pi} r_{arc}^3} \exp\left(-\frac{3[(x - x_{arc})^2 + (y - y_{arc})^2 + (z - z_{arc})^2]}{r_{laser}^2}\right) \quad (1)$$

where η_{arc} is the absorption efficiency of the arc, U is the arc voltage, I is the arc current, and r_{arc} is the heat density distribution radius of the arc. x_{arc} , y_{arc} , and z_{arc} are the coordinates of the arc center on the x , y , and z axis, respectively.

The heat distribution of the laser is described as:

$$q_{laser}(x, y) = 3 \frac{\eta_{laser} P_{laser}}{\pi r_{laser}^2 h} \exp\left(-\frac{3[(x - x_{laser})^2 + (y - y_{laser})^2]}{r_{laser}^2}\right) \quad (2)$$

where η_{laser} is the absorption efficiency of the laser and P_{laser} is the

Download English Version:

<https://daneshyari.com/en/article/8047957>

Download Persian Version:

<https://daneshyari.com/article/8047957>

[Daneshyari.com](https://daneshyari.com)